Searching for the sweet spot of amoebic gill disease of farmed Atlantic salmon: the potential role of glycan-lectin interactions in the adhesion of Neoparamoeba perurans

Author

Lima, PC, Hartley-Tassell, L, Cooper, O, Wynne, JW

Published

2021

Journal Title

International Journal for Parasitology

Version

Version of Record (VoR)

DOI

10.1016/j.ijpara.2020.11.009

Searching for the sweet spot of amoebic gill disease of farmed Atlantic salmon: the potential role of glycan-lectin interactions in the adhesion of *Neoparamoeba perurans*

P.C. Lima[a,*], L. Hartley-Tassell[b], O. Cooper[b], J.W. Wynne[c]

[a] *CSIRO Agriculture and Food, Livestock & Aquaculture, Queensland Biosciences Precinct, 306 Carmody Road, Brisbane, QLD 4067, Australia*

[b] *Institute for Glycomics, Griffith University, Gold Coast Campus, Gold Coast, QLD 4222, Australia*

[d] *CSIRO Agriculture and Food, Livestock & Aquaculture, Castray Esplanade, Battery Point, TAS 7004, Australia*

*Corresponding author. Tel.: +61 7 3410 3114. *E-mail address*: paula.lima@csiro.au

Note: Supplementary files associated with this article

Abstract

One of the first critical steps in the pathogenesis of amoebic gill disease (AGD) of farmed salmon is the adhesion of the causative amoeba to the host. The current study aimed to investigate the potential involvement of glycan-binding proteins expressed on the extracellular surface of *Neoparamoeba perurans* in gill tissue recognition and binding. The glycan-binding properties of the surface membrane of *N. perurans* and the carbohydrate binding profile of Atlantic salmon gill-derived epithelial cells were identified through the use of glycan and lectin microarrays, respectively. The occurrence of specific carbohydrate-mediated binding was then further assessed by in vitro attachment assays using microtitre plates pre-coated with the main glycan candidates. Adhesion assays were also performed in the presence of exogenous saccharides with the aim of blocking glycan-specific binding activity. Comparative analysis of the results from both lectin and glycan arrays showed significant overlap, as some glycans to which binding by the amoeba was seen were reflected as being present on the gill epithelial cells. The two main candidates proposed to be involved in amoeba attachment to the gills are mannobiose and *N*-acetylgalactosamine (GalNAc). Adhesion of amoebae significantly increased by 33.5 and 23% when cells were added to α1,3-Mannobiose-BSA and GalNAc-BSA coated plates. The observed increased in attachment was significantly reduced when the amoebae were incubated with exogenous glycans, further demonstrating the presence of mannobiose- and GalNAc-binding sites on the surfaces of the cells. We believe this study provides the first evidence for the presence of a highly specific carbohydrate recognition and binding system in *N. perurans.* These preliminary findings could be of extreme importance given that AGD is an external parasitic infestation and much of the current research on the development of alternative treatment strategies relies on either instant amoeba detachment or blocking parasite attachment.

Keywords: Amoeba, AGD, Attachment, Glycans, Mannobiose, *N*-acetylgalactosamine

1. Introduction

Host tissue adhesion and colonization is the first critical step in the pathogenesis of diseases caused by viruses, bacteria and protozoans (Bonazzi and Cossart, 2011). In most cases, this initial interaction is mediated by a highly specific carbohydrate recognition system in which glycan-binding proteins (GBPs) such as adhesins and lectins, expressed on the extracellular surface of pathogens, recognise and bind to target glyconjugate receptors on the host epithelial cells (Singh et al., 2016a).

In the case of amoeba-related diseases, adhesion is required not only for successful colonization of the host surface epithelium, but also for subsequent invasion and disease progression (Betanzos et al., 2019). Furthermore, lectin-mediated attachment is required for multiple secondary processes such as phagocytosis, apoptosis and secretion of proteases (Leher et al., 1998; Gilchrist and Petri, 1999; Panjwani, 2010; Huth et al., 2017). It has been reported that *Acanthamoeba castellanii*, the causative agent of a chronic inflammatory disease of the cornea known as *Acanthamoeba* keratitis, attaches and invades the host cells by interactions between distinct mannose-specific carbohydrate-binding proteins expressed on the surface of the amoeba and glycoproteins containing mannose residues on the surface of host corneal epithelial cells (Yang et al., 1997). Similarly, a galactose-/*N*-acetylgalactosamine (Gal/GalNAc)-binding lectin expressed on the surface of the intestinal parasitic amoeba *Entamoeba hystolytica* is required for adhesion to human colonic mucin, cytolysis and invasion (Frederick and Petri, 2005).

Humans are not the only species affected by diseases caused by amoebae. The world-wide Atlantic salmon aquaculture industry is significantly affected by a highly problematic amoeba-mediated proliferative condition known as amoebic gill disease (AGD) (Mitchell and Rodger, 2011). In Tasmania (Australia), where it was first reported in the 1980s, AGD remains one of the major health challenges faced by the local industry (Oldham et al., 2016). The disease is caused by the free-living opportunistic amoeba *Neoparamoeba perurans,* which colonises the gills of seawater reared Atlantic salmon (Crosbie et al., 2012). Colonisation of the gills by this parasite causes proliferative cell change reactions, including severe epithelial hyperplasia, hypertrophy, oedema and interlamellar vesicle formation (Adams and Nowak, 2003). In Australia, treating the disease involves bathing the fish in freshwater for 2-3 h (Parsons et al., 2001), which is not only costly (approximately $50 million/year) and time consuming, but also environmentally unsustainable, as excessive amounts of freshwater are required. Moreover, treatment strategies that directly target pathogen viability are likely prone to select for resistance (de Koning, 2017; Lamotte et al., 2017); a hypothesis which has already

been proposed in regard to freshwater bathing (Lima et al., 2017; Wright et al., 2018). As a result, the development of alternative treatment strategies that either directly or indirectly target *N. perurans* viability by interfering with mechanisms of host interactions are highly desirable (Sarabia-Sainz et al., 2013; Raval et al., 2015; Singh et al., 2016b). Therefore, a good understanding of the host-pathogen interface and recognition processes is required.

Although numerous species of amoeba have been isolated from the gills of AGD-affected salmon (Howard, 2001. Paramoebiasis of sea-farmed salmonids in Tasmania - a study of its aetiology, pathogenicity, and control. PhD dissertation, Latrobe University, Australia; Bermingham and Mulcahy, 2007; English et al., 2019), only *N. perurans* has been proven to elicit the disease (Crosbie et al., 2012). Given that the ability to invade tissues following carbohydrate-mediated attachment is considered a characteristic that distinguishes pathogenic from non-pathogenic amoebae (Da Rocha-Azevedo et al., 2009; Jamerson et al., 2012) it is possible that *N. perurans* is equipped with a surface glycan-binding protein that has the ability to recognise and access specific sugars on the host gill epithelial tissue. Transcriptomic profiling of AGD-affected gills also showed that a C-type lectin was significantly up-regulated in Atlantic salmon immediately after AGD infection (Morrison et al., 2006). The observed up-regulation remained during the first 5 days p.i., suggesting the potential recognition of amoeba glycan epitopes by the host. The existing evidence on the possible role of lectin-glycan interactions between *N. perurans* and Atlantic salmon has been reviewed by Nowak et al. (2014). Surprisingly, no additional information on this topic have been published since then. The relevant literature will be further discussed in this study to support our main findings.

The current study aimed to determine the glycan-binding properties of the surface membrane of *N. perurans* and the carbohydrate profile of gill epithelial cells through the use of glycan and lectin microarrays, respectively. The *N. perurans* pseudocyst (Lima et al., 2017) was employed as a control, given that gill-specific carbohydrate-binding sites should not be expected on the cell membrane of this dormant and exclusively floating stage. Further surface plasmon resonance (SPR) analysis and in vitro adherence assays were also employed to validate the role of specific glycans on the ability of *N. perurans* to attach. To our knowledge this is the first study exploring the use of glycan and lectin microarrays to investigate adhesion mechanisms of *N. perurans*.

2. Materials and methods

104 *2.1. Neoparamoeba perurans strains*

105 The *N. perurans* isolate employed in this study was the MP2 strain isolated and characterised by
106 English et al. (2019). The amoebae were grown in 25 cm^2 Nunc™ culture flasks (Thermo Fisher
107 Scientific™, EUA) overlaid with 1% malt yeast broth (0.01 % (w/v) malt extract (Thermo Fisher
108 Scientific™ Oxoid™) and 0.01 % (w/v) yeast extract (Thermo Fisher Scientific™ Oxoid™) in 33 ppt filtered
109 sterile seawater), as previously described (English et al., 2019). The age of the culture at the time it was
110 harvested for the assays was 18 months. Even though, at that time, it was uncertain to whether MP2 was still
111 infective to fish, the same strain was later (at 23 months old) successfully employed to elicit amoebic gill
112 disease (AGD) in naïve Atlantic salmon during a controlled in vivo trial (English et al., 2021). Prior to each
113 assay, the 10 ml monolayer of amoebae was harvested by tapping culture flasks against a hard surface and
114 flushing using a transfer pipette. Amoebae cells were then transferred to 15 ml Corning™ Falcon™ tubes
115 (Thermo Fisher Scientific™), pelleted by centrifugation (10,000 *g*, 30 min, 16°C), and resuspended in sterile
116 seawater before a further centrifugation step. The final pellet was re-suspended in 1 ml of seawater and cells
117 enumerated by haemocytometer counts.

118

119 *2.2. Cell labelling*

120 In vitro cultured amoeba cells were labelled with Bodipy TR methyl ester dye (Thermo Fisher
121 Scientific™) prepared to 1 mM in sterile MilliQ water. To avoid osmotic stress, cells were maintained in
122 sterile seawater (33 ppt) and labelled at a final concentration of 2 µM of dye, for 30 min, at room
123 temperature. Labelled cells were then washed three times by centrifugation to remove excess dye, fixed in
124 4% formaldehyde (Sigma-Aldrich, German) for 20 min and re-suspended in seawater.

125 Freshwater-induced pseudocysts (Lima et al., 2017) were employed as controls given that gill-
126 specific binding sites should not be expected on the surface of this dormant and non-adherent stage of *N.*
127 *perurans*. Labelled pseudocysts were generated by submitting pre-labelled floating cells to 10 min
128 incubation in freshwater, followed by centrifugation (1000 *g*, 5 min, 16°C). Pelleted labelled pseudocysts
129 were then fixed as above and re-suspended in MilliQ water.

130 Gill epithelial cells were scavenged from one humanely euthanised naïve Atlantic salmon reared at
131 the Bribie Island Research Centre (Queensland, Australia), as per Exemption EX 2020-03 approved by the
132 CSIRO Queensland Animal Ethics Committee, Australia. The gill basket was removed, thoroughly rinsed in

sterile seawater to remove excess blood and the gill arches were carefully scraped using a cell scraper to eliminate the overlaying mucus layer. The gill filaments from one arch were then excised and homogenised through a 100 µm Corning® cell strainer (Merck, Germany). Cells were washed several times in sterile seawater and inspected under a microscope to confirm epithelial morphology. A small number of different cell phenotypes was found; however, target cells were clearly the dominant type. Cell labelling and fixation was performed as described above for the amoebae.

For flow cytometry, both labelled and unlabelled cells were diluted in PBS to contain approximately 20,000 cells per ml. Side scatter and forward scatter were adjusted for each cell population, and the fluorescence of FL-3 Texas Red –PE measured at 595 nm. Cell populations were gated and plotted using FloJo version 10 (Tree Star, Ashland, United States). The samples containing epithelial cells were also checked at 647 nm to confirm successful removal of blood cells.

2.3. Glycan array on amoeba and pseudocyst cells

Glycan arrays were performed as previously described by Day et al. (2009). Briefly, 415 glycans were printed at a concentration of 500 µM using an ArrayJet Marathon Argus non-contact printer (ArrayJet Ltd., United Kingdom), whereby four drops per spot were printed in quadruplicate onto an OPEpoxy glass slide (Capital Bio, China). The full list of glycans printed on the array is shown in Supplementary Table S1. Approximately 10,000 labelled amoeba cells were diluted into a final volume of 300 µL in array PBS (PBS with 1.8 mM $MgCl_2$/$CaCl_2$) and placed onto the slide without a coverslip for 15 min in the dark. The slide was then immersed in array PBS and washed gently for 5 min.

The slide was then scanned using an InnoScan 1100AL (Innopsys, France) microarray scanner, using the 488 nm, 532 nm and 635 nm lasers, low laser power and 50% photomultiplier (PMT) gain settings. The acquired image was then analysed using the Mapix software (Innopsys), overlaying the image with the map GenePix Array List (GAL) file. The experiment was repeated three times, and binding was classified as positive when the average relative fluorescence unit (RFU) of a specific structure had a value above mean background (defined as the average background fluorescence plus 3 S.D.), and a P value of < 0.005 (student's t-Test). Supplementary Table S2 documents the glycan microarray based on the minimum information required for a glycomics experiment (MIGAGE) (Liu et al., 2016).

161

162 *2.4. Lectin arrays on gill epithelial cells*

163 Lectin arrays were prepared as previously described by Semchenko (2012). The lectin array
164 consisted of 90 commercially available (Supplementary Table S3) carbohydrate-binding proteins, most with
165 characterised binding profiles. Although the specificities of the lectins have been determined, this is
166 normally done using simple monosaccharides. This method has shown that each lectin can have different
167 affinities for various monosaccharides, and in some cases a diverse glycan-binding profile. For this reason,
168 multiple lectins with similar binding patterns were printed, in order to provide more information on glycan
169 structures in terms of linkage, position and neighbouring glycan. Briefly, each lectin was printed at 1:2
170 dilutions from 125 to 500 µg/ml in quadruplicate spots on OPEpoxy glass slides (Capital Bio), using a non-
171 contact Arrayjet Marathon Argus microarray printer (ArrayJet Ltd.). Prior to use, slides were blocked using
172 1% BSA in PBS on ice for 2 h. Slides were then rinsed in PBS and dried by centrifugation at 200 *g* for 4
173 min.

174 Labelled epithelial gill cells were diluted 1:3 using array PBS, to a final volume of 400 µl. The cells
175 were incubated on the array for 30 min in the dark. After the incubation time, the slide was immersed in
176 array PBS and washed gently for 4 min. The slide was then transferred to a clean 50 ml tube and dried by
177 centrifugation at 200 *g* for 4 min. The slide was scanned using the Innoscan 1100AL (Innopsys) microarray
178 scanner, using the 605/611 ex/em filter fitted on the 532 nm laser. The image was acquired using low laser
179 power and 50% PMT gain settings. The acquired image was analysed using Mapix analysis software
180 (Innopsys), whereby a map (GAL) file was overlayed on the acquired image. The experiment was repeated
181 three times. Table 1 provides a full list of lectins printed on the array and their respective binding specificity.
182 Binding was deemed positive as per the glycan array. Supplementary Table S4 documents the lectin
183 microarray according to MIRAGE (Liu et al., 2016).

184

185 *2.5. Surface plasmon resonance (SPR)*

186 SPR analysis was employed to further investigate the binding interactions between the amoeba
187 surface and selected glycans. Seventeen glycans were chosen based on the results from the glycan and lectin
188 microarrays (Table 2) and comprised structures containing: mannosyl (5D, 5E, 5F), terminal galactose (1A,
189 1E), ganglioside (17G, 17N), sialic acid (10B), fucose (fuc) (7I, 19J, 7F, 7K, 8P, 20B, 18E, 7O) and *N*-

acetylgalactosamine (GalNAc) (2C). Structures comprising GalNAc were also present in some of the selected Blood Group glycans (i.e 7K, 8P, 20B and 18E). Whole cell-carbohydrate interaction studies were performed using a GE Healthcare BIAcore™ T200 instrument (BIAcore, Sweden). A Series S C1 sensor chip (GE Healthcare, United States) was used for all experiments, whereby the amoeba cells were immobilized onto the C1 chip by amine coupling. The running buffer (PBS) was filtered through a 0.22 µm filter prior to being degassed by sonication. All glycans were resuspended in running buffer at concentrations 1 nm - 10 µM.

2.5.1. Immobilisation of amoeba cells

Briefly, the isolated amoebae were diluted into 10 mM sodium acetate buffer (Sigma-Aldrich), pH 4.5. For amine coupling, the carboxylmethylated matrix-free surface of the sensor was first cleaned with 100 mM glycine (Sigma-Aldrich) with 0.3% triton-100 (Thermo Fisher Scientific™) pH 12.2, followed by activation using a 30 µl (6 min) injection of a mixture of 0.2 M 1-ethyl-3-[(3-dimethylamino)propyl]-carbodiimide (EDC) (Sigma-Aldrich) and 0.05 MN-hydroxysuccinimide (NHS) (Sigma-Aldrich), which resulted in the conversion of carboxyl groups to an NHS ester. The cells then were poured over the surface for 2100 s at a flow rate of 5 µl/min and immobilised through the amide linkage. The remaining unreacted NHS ester groups were neutralised by 30 µl of 1 M ethanolamine-HCl (Sigma-Aldrich) (pH 8.0). Under these conditions, 300 response units (RU) of amoeba were immobilized. The reference surface (Fc1) underwent the same treatment, without sample injection.

2.5.2. Determination of interaction affinities

Whole cell-carbohydrate interaction studies were carried out in PBS (pH 7.3) at a flow rate of 30 µl/min, at 25°C. The glycans listed in Table 2 were analysed using single cycle kinetics at concentrations between 1 nm and 10 µM, depending on the affinity data. Kinetic data could not be determined due to the nature of small molecule interactions. For each glycan, several buffer-only injections were run prior to and after each single-cycle run, to ensure complete regeneration of the surface.

2.5.3. Data analysis

SPR data was analysed using BIAcore T200 evaluation software 3.0 (GE Healthcare). Sensorgrams were automatically XY-zeroed and subtracted against the reference cell (2-1, 3-1, 4-1) and furthermore the blank/buffer reference was subtracted. Double reference subtracted sensorgrams for each of the glycans are shown in Supplementary Fig. S1. The dissociation equilibrium constant (K_D) values between the ligand and each analyte were determined by steady state affinity, whereby the data was plotted and the predicted maximum binding response (R_{max}) determined. Theoretically, R_{max} is reached as the analyte binding capacity of the ligand surface is saturated. Table 2 lists the glycans and their associated affinities, R_{max} and chi^2 values.

2.6. Adherence assays

Mannobiose and GalNAc were selected for further validation using an in vitro solid-phase attachment assay. These two glycans were chosen based on: i) the correlations made between glycan and lectin microarrays; ii) the SPR analysis binding affinities; iii) a mannose-binding protein similar to the one expressed on the surface of the parasitic amoeba *A. castellanii,* was identified for *N. perurans* (Valdenegro-Vega et al., 2014); and iv) antibodies that bind the Gal/GalNAc inhibitable lectin of *E. histolytica* also bound to live wild-type *Neoparamoeba* spp. (Vincent, 2008. Amoebic gill disease of Atlantic salmon: resistance, serum antibody response and factors that may influence disease severity. PhD dissertation, University of Tasmania, Australia). The in vitro adhesion assay was adapted from Caot et al. (1998) and Yang et al. (1997). Briefly, 96 opaque-walled microtiter plates (Corning®, United States) were pre-coated with 100 µl aliquots of either α1,3-Mannobiose-BSA (MNB-BSA) or GalNAC-BSA diluted in 0.1 M sodium carbonate buffer (1 µg/ml), pH 9.6. These neoglycoproteins were purchased from Dextra Laboratories Ltd. (United Kingdom) and contained 15–30 mol of sugar/mol of albumin. BSA-coated wells (1% in PBS) were included as controls to assess non-specific attachment and each treatment was performed in quadruplicate. Amoeba pre-incubation in BSA solution was attempted as an additional control; however, the cells developed into an irregular floating blob and, consequently, could not be employed in the assay. Coating was performed at 4°C overnight, followed by rinsing with PBS. Non-specific binding was blocked with 1% BSA in PBS (1 h, room temperature) prior to adding *N. perurans* cells into respective wells (5000 cells/well in seawater). Following a 60 min incubation at 16 °C, wells were washed twice with sterile seawater to remove unbound cells and a fresh 100 µl layer of sterile seawater was added to each well. Attached amoebae were then assessed using the

CellTiter-Glo® Luminescent Cell Viability Assay Kit (Promega, United States), which is designed to determine the number of metabolically viable cells based on the quantity of ATP being produced in each replicate (Botwright et al., 2020). For this purpose, 100 µl of CellTiter-Glo® Reagent (Promega) were incorporated into each well, followed by 2 min mixing on an orbital shaker to induce cell lysis. Plates were then incubated at room temperature for 10 min and the luminescence signals of the solubilised solutions determined with a SpectraMax M3® Multi-Mode Microplate Reader (Molecular Devices, United States). Assays were performed in triplicate.

2.7. Competitive adherence assays

To determine the ability of exogenous saccharides to bind to, and therefore block, specific binding sites on the amoeba surface, the adherence assay was repeated in the presence of free mannose and GalNAc (Sigma-Aldrich). A sucrose (Suc) treatment was included as a control. In brief, 5000 amoeba cells/replicate were pre-incubated with 100 mM of each saccharide for 60 min at 16°C. Following the incubation period, the amoeba cells were then washed in sterile seawater and transferred to coated wells. The adhesion assay was performed and analysed as described in section 2.6.

2.8. Statistical analysis

Differences in amoeba attachment levels within treatments were calculated by one-way analysis of variance ANOVA followed by Tukey's post-hoc test, using GraphPad Prism 8.3.1 (United States). A Kolmogorov–Smirnov test was employed to check for normal distribution and Bartlett's test for constancy of variances. Values were considered to be significant at $P < 0.05$. All numerical data were expressed as the mean ± standard error.

3. Results

3.1. Cell labelling and flow cytometry

As shown in Fig. 1A-C, all cell types, amoeba, pseudocyst and gill, were successfully labelled using the lipophilic Bodipy595-ME dye. The unlabelled cells did not show any auto-fluorescence using the 488 nm, 532 nm (555 and 595 nm) or the 635 nm lasers. Effective labelling was also confirmed using flow cytometry by overlaying the peaks of labelled and unlabelled populations. Clear separation between labelled

and unlabelled samples was observed for the gill epithelial cells (Fig. 1C). Even though a similar level of fluorescence was detected for the amoeba and pseudocyst samples, the intrinsic fluorescence detected for labelled cells was high enough to differentiate both populations (Fig. 1A-B). Effective removal of blood cells was confirmed at 647 nm, which is the expected wavelength to detect this cell type.

3.2. Glycan Array Analysis of amoeba and pseudocyst

A total of 104 distinct glycan structures, covering 11 main classes, were significantly bound by the amoeba. The dormant floating stage of *Neoparamoeba perurans*, on the other hand, presented significant binding to only five glycans. Fucosylated glycans were the most representative structures bound by the amoeba cells, with almost a quarter (21) of the positive binding hits detected within this class of carbohydrates. Glycans containing β-galactose terminal structures (19) were the second most bound by *N. perurans*. The remaining positive binding consisted of structures containing mannosyl (8), glucoromyl (8), gangliosides (7), glycosaminoglycan (6), glycosaminoglycan disaccharides (8), sialylate (9) and terminal *N*-acetylgalactosamine (GalNAc) (3), α-galactose (6) and N-Acetylglucosamine (9). Out of the five glycans bound by the floating pseudocysts, only two, one with mannosyl (Man6P (47)) and another with terminal β-Galactosyl (LNT (376)) structures, were bound by both cell types. However, unlike amoeba trophozoites, which bound to several different structures containing mannose and β-galactose, pseudocysts only showed significant attachment to one of each. This was also apparent with terminal N-Acetylglucosamine structures, as only GlcNAc-Mur (167) was bound by the pseudocysts, whereas a larger range of this class showed interaction with amoeba trophozoites. The full list of glycans printed onto the array slides are given in Supplementary Table S1. Table 3 indicates in red the glycans bound by the amoeba and pseudocyst cells.

3.3. Lectin Array Analysis of gill epithelial cells

Based on the lectin binding profile obtained by the array, it is possible to suggest that glycan structures containing Manα1-3Man (terminal) are present on the gill epithelial surface. This is due to the binding of ASA, CPA, HHA, LcHB, GNA, NPA, PEA, VFA and VVA-man. Terminal GalNAcα1-3GalNAc/Gal is another likely structure, as shown by the binding of CSA, SSA, DBA, GHA, HAA, IRA, TL and WFA. The presence of GlcNAcβ1-4GlcNAc is also suggested as gill cells showed positive binding to LAA, LEA, UDA and UEA-II. Since binding was not seen for ABA, ACA and VGA, it is unlikely that the

binding receptor is a Galβ1-3GalNAc, which is also bound by PNA. However, given that both VAA and PNA showed positive binding, the presence of Galβ1-4Glc could also be suggested. One trisaccharide, Galβ1-4GlcNAcβ1-2Man, was detected by PHA-L. Interestingly, only one lectin (SNA-I) indicated the presence of sialylated glycan, which suggests that a structure terminating in Neu5Acα2-6Gal, Neu5Acα2-6GalNAc is also present on the gill cells. One lectin with α-galactose (α-gal) affinity (VRA) was also detected. Table 1 lists the lectins printed on the array slides and highlighted in red are those that showed positive binding to labelled gill cells.

3.4. SPR analysis

The two glycans that showed the highest binding interaction with *N. perurans* were 2C (9 nM) and 5D (12.4n M), which contain terminal GalNAc (GalNAcβ1-3Gal) and mannosyl (Manα1-3Man) structures, respectively. The chi^2 values for both of these interactions were below 10% of the respective $R_{max,}$ and, therefore, were considered within the "good fit" range. However, the R_{max} for 5D (1.4 RU) was considerably lower than for 2C (4.7 RU), indicating that less Manα1-3Man binding sites are required on the amoeba surface to achieve saturation of the related analyte. The other two mannose-containing glycans (5E and EF) also showed binding by the amoeba, but with lower affinity (121.5 and 114.3 nM) and higher R_{max} values (5.4 and 2.1 RU). Apart from 8P (Blood Group A tetrasaccharide), all other glycans containing GalNAc (1E, 7K, 20B and 18E) were also bound by the amoeba, with K_D values ranging from 59.7 to 125.7 nM. Interestingly, 1E (Galβ1-3GalNAc) is the reverse structure of 2C, but a six-fold higher nanomolar affinity was observed for this structure. With regard to the fucosylated glycans, the two with highest affinity interactions were 7O (Fucα1-2Galβ1-3GlcNAc) and 19J (Galβ1-4(Fucα1-3)GlcNAcβ1-3Gal). Similar K_D (17.4 and 21.6 nM) and R_{max} (4.3 and 4.5 RU) were detected for these glycans. Positive binding was also recorded for the two selected gangliosides, GM1b (17G, 65.6 nM) and GD3 (17N, 69.1 nM), but the observed affinity was approximately seven times weaker than for the glycan with highest interaction (2C, 9 nM). The sialylated glycan (10B), on the other hand, recorded the fifth strongest interaction (32.3 nM) out of the seventeen selected glycans. The K_D, R_{max} and chi^2 values for each glycan are shown in Table 2, with glycans scored with the smallest K_D values regarded as the ones with the greatest binding affinity to the amoeba surface. Related sensorgrams are found in Supplementary Fig S1.

334 *3.5. Adherence and competitive assays*

335 Comparative analysis of the results from both the lectin and glycan arrays showed significant
336 overlap, as some of the glycans to which binding was seen by the amoeba were reflected as being present on
337 the gill epithelial tissue. The two classes of glycans most likely to be involved in amoeba-gill interactions are
338 mannobiose and GalNAc. To further validate the ability of *N. perurans* to selectively bind to these structures,
339 individual wells of 96-well microtiter plates were coated with man-BSA and GalNAc-BSA, and the ability of
340 amoebae to attach was assessed using the CellTiter-Glo® Luminescent Cell Viability Assay. The assay
341 determines the number of viable cells by quantifying the amount of ATP being produced in a given replicate.
342 Therefore, the higher the luminescence, the higher the number of attached cells present in the well.
343 According to the viability assay, the number of amoebae bound to α1,3-Mannobiose-BSA- (MNB-BSA-)
344 and GalNAc-BSA-coated wells significantly increased by approximately 1.8 and 1.6-fold (P <0.005),
345 respectively, compared with the BSA-only substrate (Fig. 2A and B). The addition of free mannose and
346 GalNAc to the culture media successfully reduced the specific glycan-mediated adhesion by 31.74 ± 5.61%
347 and 30.88 ± 6.08%, respectively (Fig. 2A and B). Even though only a partial inhibition was observed, the
348 average attachment level in the presence of exogenous mannose or GalNAc was similar to the BSA control
349 (Fig. 2A and B). As expected, amoebae binding to MNB-BSA- and GalNAc-BSA-coated wells was not
350 affected by the presence of exogenous Suc (Fig. 2A).

351

352 **4. Discussion**

353 Glycan and lectin microarrays have emerged as powerful tools for determining the ligand
354 specificities of glycan-binding proteins (GBPs) involved in host-pathogen adhesion (Smith and Cummings,
355 2014; Huang et al., 2015; Kim et al., 2018). Glycan microarrays consist of individual glycan structures
356 immobilized on a well-defined substrate in a spatially defined arrangement. This creates a multivalent ligand
357 display that can elicit sufficiently strong binding by GBPs. Labelled proteins, cell surface receptors or whole
358 pathogens are then added to printed glycans spots and binding is quantified via fluorescence-based detection
359 methods. Lectin microarrays, on the other hand, employ the same principle but using immobilized lectins
360 with known glycan specificity to assess the glycan patterns present on the surface of labelled molecules (Hu
361 and Wong, 2009).

In the current study, glycan and lectin microarrays were employed to identify potential candidates involved in specific carbohydrate-mediated attachment of *Neoparamoeba perurans* to Atlantic salmon gills. The glycan array performed on labelled *N. perurans* cells identified which glycan structures the amoebae bound to, whereas the lectin array indicated the glycan structures present on the surface of gill epithelial cells. The comparison of the results between the lectin and glycan arrays showed significant overlap as a series of glycans bound by the amoebae were also detected on gill epithelial cells. However, it is important to consider that a small number of non-target cells was observed within the gill epithelial samples and that these could possibly have elicited a false positive. Still, we are confident that in diluted samples these cells were not present in high enough numbers to result in a significant relative fluorescence unit (RFU) reading. In fact, some of the lectins printed on the array did elicit minor, but not significant, binding which could be that of non-target cells. In the current paper, all statistically significant binding on the lectin array has been deemed as that of gill epithelial cells.

Mannobioses are disaccharide glycan structures formed by two mannose molecules with varying glycosidic linkages (Pendrill et al., 2019). The lectin array indicated that mannobiose (Manα1-3Man)-containing glycans were present on the gill epithelia. Similarly, the glycan array showed significant amoebae binding not only to Manα1-3Man structures, but also to biantennary N-linked core pentasaccharide and complex N-type glycans, which also have terminal Manα1-3Man structures at the end. Most importantly, Manα1-3Man (3D) was also the glycan with the second highest binding affinity according to the surface plasmon resonance (SPR) analysis. This glycan also showed the lowest R_{max} value, which indicates that only very small amounts of Manα1-3Man binding sites would be required on the gill surface for the amoeba to successfully attach. The ability of *N. perurans* to bind to Manα1-3Man was further validated in vitro using α1,3-Mannobiose-BSA- (MNB-BSA)-coated microplates. The presence of specific mannose-binding sites on the surface of the amoeba was also confirmed by pre-incubating *N. perurans* cells with free mannose, which inhibited the initially observed MNB-dependent increment in adhesion. Adhesion of *Acanthamoeba castellanii* to corneal epithelial cells, a key first step in the pathogenesis of *Acanthamoeba* keratitis (AK), is mediated by a mannose-binding protein (MBP) (Panjwani, 2010). Interestingly, a MBP-like factor, similar to attachment factors of *Acanthamoeba* spp., has been identified in the transcriptome of *N. perurans* (Valdenegro-Vega et al., 2014). Anti-MBP antibodies produced in Atlantic salmon serum and mucus also bound to the external surface of fixed *N. perurans* trophozoites (Valdenegro-Vega et al., 2014), further

demonstrating the potential role of host mannose in amoeba interaction. The presence of mannose structures on the surface of the amoeba, on the other hand, has been proposed to play a role in host immune response evasion (Morrison et al., 2006). According to the authors, significant downregulation of a MBP-C was reported in the transcriptome of amoebic gill disease- (AGD)-affected gills of Atlantic salmon, at 189 h p.i. (Morrison et al., 2006). The studies above suggest that mannose could play a role not only in initial cell adhesion and recognition processes, but also in subsequent immune evasion mechanisms.

As observed in this study, inhibition of *Acanthamoeba* sp. attachment to rabbit corneal epithelium was also observed in the presence of exogenous mannose (Yang et al., 1997). The inhibitory effect varied from 38% at the lowest (0.01 M) to 84% at the highest (0.2 M) concentration tested. Given that higher doses of saccharide were employed in comparison to the present study (100 mM), it is expected that the observed binding reduction of approximately 30% could be increased if higher doses of exogenous glycan were to be employed. Mannose receptors are also known to be involved in the attachment mechanism of pathogenic yeast (Yan et al., 2020) and bacteria (Kim et al., 2018).

Another potential candidate involved in attachment of *N. perurans* to Atlantic salmon gills is *N*-acetylgalactosamine (GalNAc), as amoeba cells significantly bound to the O-glycan core structure, core 5, and GalNAcα1-3GalNAc glycan, and results from the lectin array indicated that this structure was also present on the gill epithelial cells. Terminal GalNAcβ structures are also expected on the cell membrane of gill epithelial cells and, according to the glycans array, *N. perurans* showed significant binding to GalNAcβ1-3Gal (2C). Most importantly, 2C was the glycan with the strongest binding affinity to the amoeba surface, which reinforces the role of GalNAc in *N. perurans* adhesion to salmon gills. Once again, the solid-phase and competitive in vitro assays using GalNAc-BSA-coated substrate confirmed the positive binding interaction between the amoeba and this glycan. Similarly, the causative agent of amoebiasis in humans, the protozoan amoeba *Entamoeba histolytica*, colonizes the mucus layer of the colon by adhering to mucin oligosaccharides by means of a galactose/*N*-acetyl *D*-galactosamine (Gal/GalNAc)-lectin (Frederick and Petri, 2005). Either monoclonal antibodies that bind to the *E. histolytica* Gal/GalNAc lectin, galactose or GalNAc have been demonstrated to block lectin-mediated attachment of *E. histolytica* to target carbohydrate residues (Ravdin and Guerrant, 1981; Ravdin et al., 1986, 1985; Burchard and Bilke, 1992). One result that suggests that GalNAc, but not galactose, is involved in *N. perurans* binding to salmon gills was demonstrated by Vincent (2008. Amoebic gill disease of Atlantic salmon: resistance, serum antibody

response and factors that may influence disease severity. PhD dissertation, University of Tasmania, Australia). The author showed that monoclonal and polyclonal antibodies that bind to the *E. histolytica* Gal/GalNAc lectin bound to the surface of live wild-type *Neoparamoeba* spp., however, the presence of exogenous galactose enhanced, rather than inhibited, antibody binding. The amoeba floating pseudocyst stage showed no binding to either mannobiose or GalNAc structures, reinforcing the potential role of these glycans in *N. perurans* attachment. Moreover, the fact that the amoeba pseudocysts bound to only five glycan structures, as opposed to the 104 observed for the trophozoites, further validates a previous hypothesis that the *N. perurans* pseudocyst is an inactive stage (Lima et al., 2017).

Even though the lectin array indicated that only one sialylated glycan structure is present on the gill epithelial cells, several gangliosides, some of which were also bound by the amoeba in the glycan array and SPR analysis, have been isolated from the gills of Pacific salmon, *Oncorhynchus keta* (Niimura, 2006). Given that gangliosides are sialic acid-containing glycosphingolipids (Yu et al., 2011), the role of these glycan structures on *N. perurans* attachment to Atlantic salmon gills should not be ruled out. Moreover, infectious salmon anaemia virus (ISAV), which also affects farmed Atlantic salmon, attaches to the host via sialic acid-containing receptors and studies suggest that gills are the point of entry for ISAV (Aamelfot et al., 2012; Weli et al., 2013).

Albeit fish are known to not express galactose-alpha-1,3-galactose (α-gal) (Macher and Galili, 2008; Kollmann et al., 2017), a lectin with α-gal specificity (VRA) showed significant binding to the gill epithelial cells. However, considering the field of glycobiology is mostly focused on mammalian glycosylation, the presence of α-gal Atlantic salmon gills should not be disregarded. If that is the case, α-gal could also be regarded as an adhesion candidate as multiple terminal α-gal structures were bound by *N. perurans* in the glycan array.

Repeating N-acetyl glucosamine (GlcNAc) structures were bound by the amoeba and found to be present on the gill cells. However, the structures on the epithelial cells are more likely to be long repeating pentasaccharide units rather than the shorter disaccharides bound by the amoeba in the glycan array. As a result, it is unlikely that amoeba attachment to the gill is mediated by GlcNAc-binding. Similarly, glucose is not expected to be involved in *N. perurans* attachment to the host, as lectins with glucose affinity, such as ConA, did not show significant binding on the lectin array. The binding to glycosaminoglycans (GAGs) is also likely to be non-specific, as GAG structures are long polymers that are highly negatively charged due to

449 sulfation (Gandhi and Mancera, 2008), and this charge may contribute to the amoeba attachment since
450 *Neoparamoeba* spp. require negatively charged substrate for non-specific adhesion (Martin, 1987).
451 Moreover, GAG structures are found in the extracellular matrix and, as such, are not specific to particular
452 cells types (Yamada et al., 2011). If the gill is the only site of attachment of the amoeba, it is highly probable
453 that this attachment is not mediated by a common and widely dispersed glycan structure.

454 Although there was extensive binding to 21 fucosylated structures by the amoebae, the lectin array
455 indicated they were not present on the gill epithelia of naïve fish and, therefore, were unlikely to play a role
456 in gill colonization. However, according to Marcos-López et al. (2017), terminal α-L-fucose is one of the
457 most abundant glycans present on gill mucus of Atlantic salmon. The epithelial surface of fish gills is
458 covered by a mucus layer which is the front-line defensive barrier between external stressors and the host
459 (Reverter et al., 2018). Given that amoebae are likely required to overcome this mucus layer before accessing
460 and colonising the underlying epithelia, it is suggested that binding to fucosylated structures present in
461 mucus could be the initial point of contact between *N. perurans* and the host. In fact, a recent study by our
462 group demonstrated that incubation with free fucose significantly reduced the ability of *N. perurans* to bind
463 to non-fish-derived mucin (unpublished results), the most abundant component in mucus (Ángeles Esteban,
464 2012). Therefore, further research is desirable to elucidate the mechanisms involved in this initial amoeba-
465 mucus interaction, as well as the prospective role of fucose structures as target binding sites in mucus. For
466 example, the lectin array should be employed to characterise the lectin binding profile of intact gill mucosa
467 and, therefore, confirm potential matches with any fucosylated structures bound by the amoeba cells. Mass
468 spectrometric analysis could also be carried out to compare and characterize the glycosylation profile of gill
469 mucus isolated from naïve and AGD-affected salmon. In vivo studies are also essential.

470 Interestingly, *N. perurans* binding was also detected in wells coated with BSA, which is frequently
471 employed in adhesion assays as a non-specific blocking agent (Abdallah and Ros, 2013). As a result, it is
472 expected that other binding mechanisms, rather than non-specific or glycan-dependent ones, are present in *N.*
473 *perurans*. For example, the ability of the amoeba *Dictyostelium discoideum* to bind to diverse hydrophobic
474 and hydrophilic surfaces (including BSA-treated glass) was suggested to occur via van der Waals attraction
475 between glycoproteins on the surface of the cell and the underlying substratum (Loomis et al., 2012).
476 Different surface membrane molecules were also proposed by Imbert-Bouyer et al. (2004) to be involved in
477 the capacity of *Acanthamoeba* sp. to bind to inert surfaces such as plastic.

One of the main limitations of our study is the fact that results from glycan arrays and SPR analysis are based on a single *N. perurans* isolate. Even though the strain is still infective (English et al., 2021), it would be interesting to investigate whether variation in binding affinity to the same target receptor (by SPR analysis) would differ amongst strains with pathogenic variability. For instance, it has been reported for *A. castellanii* that the expression levels of MBP directly correlate with the virulence potential of isolates with different degrees of in vitro pathogenicity (Garate et al., 2006). However, due to the high cost of running glycan arrays and SPR analysis we were unable to employ the methods on multiple strains. Another point to be considered is that the glycosylation profile of cells that have been kept under in vitro culture conditions for prolonged periods may diverge from those freshly isolated from the host. However, it is important to highlight that running glycan arrays on recently isolated amoebae would not be practical. Given the great variety of amoeba species found on the gills of AGD-affected Atlantic salmon (English et al., 2019), the establishment and upscaling of monocultures, followed by appropriate species identification, would be required prior to running the assays. An alternative would be to employ amoeba cells freshly harvested from Atlantic salmon gill cell lines (Cano et al., 2019). Despite the limitations, the data presented in this study are still of great value to the research community, especially taking into consideration that previous literature supports the possible role of mannose and/or GalNAc in *N. perurans*-host interactions.

In conclusion, the present study investigated the potential involvement of lectin-glycan interactions in *N. perurans* primary attachment to the gills of naïve Atlantic salmon. Even though a few glycan candidates were suggested and two of them were validated using in vitro adhesion assay, further research using gill cell lines or live fish are required to confirm the involvement of these glycans in amoeba attachment and subsequent AGD development. It is also important to consider that gill filaments are complex structures and that the intricacy of the gill epithelial glycome might not have been well represented by the employed lectin array. Additionally, the fact that *N. perurans* showed such an extensive glycan binding profile could point towards an intricate host-parasite relationship that involves, for example, complex receptor structures and/or multivalent interactions. Therefore, the investigation of the glycosylation profile of AGD-affected gill and mucus cells is desirable as it could provide valuable insights on amoeba invasion and host evasion mechanisms, as well as on underlying biological, biochemical and immunological components that confer a protective response in the host animal. To our knowledge this is the first time lectin and glycan microarrays have been employed to investigate the interaction of host-pathogens in the field of aquaculture.

Such findings will greatly facilitate further research on the development of alternative treatment strategies that involved manipulating lectin affinity and regulating amoeba adherence and/or virulence.

Acknowledgements

This work has been funded by the Joint Ridley/CSIRO Aquaculture Post-Doctoral Program, Australia. Authors would like to thank Ms Natasha Botwright for proof-reading the manuscript and the CSIRO Animal Research Ethics Committee for approving the use of one humanely killed salmon for this study (EX 2020-03).

References

Aamelfot, M., Dale, O.B., Weli, S.C., Koppang, E.O., Falk, K., 2012. Expression of the infectious salmon anemia virus receptor on Atlantic salmon endothelial cells correlates with the cell tropism of the virus. J. Virol. 86, 10571–10578.

Abdallah, B.G., Ros, A., 2013. Surface coatings for microfluidic-based biomedical devices. In: Li, X., Zhou, Y. (Eds.), Woodhead Publishing Series in Biomaterials. Woodhead Publishing, Oxford, Cambridge, and Philadelphia, pp. 63-99.

Adams, M., Nowak, B.F., 2003. Pathology of amoebic gill disease in Atlantic salmon (*Salmo salar* L.). J. Fish Dis 26, 601–614.

Ángeles Esteban, M., 2012. An Overview of the immunological defenses in Fish Skin. ISRN Immunol. 2012, 1–29.

Bermingham, M.L., Mulcahy, M.F., 2007. *Neoparamoeba* sp. and other protozoans on the gills of Atlantic salmon *Salmo salar* smolts in seawater. Dis Aquat Organ. 76, 234–240.

Betanzos, A., Bañuelos, C., Orozco, E., 2019. Host invasion by pathogenic amoebae: epithelial disruption by parasite proteins. Genes (Basel). 10, 618.

Bonazzi, M., Cossart, P., 2011. Impenetrable barriers or entry portals? The role of cell-cell adhesion during infection. J. Cell Biol. 195, 349–358.

Botwright, N.A., Rusu, A., English, C.J., Hutt, O., Wynne, J.W., 2020. A high throughput viability screening method for the marine ectoparasite *Neoparamoeba perurans*. Protist 171, 125773.

Burchard, G.D., Bilke, R., 1992. Adherence of pathogenic and non-pathogenic *Entamoeba histolytica* strains to neutrophils. Parasitol. Res. 78, 146–153.

536 Cano, I., Taylor, N.G., Bayley, A., Gunning, S., McCullough, R., Bateman, K., Nowak, B.F., Paley, R.K.,
537 2019. In vitro gill cell monolayer successfully reproduces in vivo Atlantic salmon host responses to
538 *Neoparamoeba perurans* infection. Fish Shellfish Immunol. 86, 287–300.
539 Caot, Z., Jefferson, D.M., Panjwani, N., 1998. Role of carbohydrate-mediated adherence in cytopathogenic
540 mechanisms of Acanthamoeba. J. Biol. Chem. 273, 15838–15845.
541 Crosbie, P.B.B., Bridle, A.R., Cadoret, K., Nowak, B.F., 2012. In vitro cultured *Neoparamoeba perurans*
542 causes amoebic gill disease in Atlantic salmon and fulfils Koch's postulates. Int. J. Parasitol. 42,
543 511–515.
544 Da Rocha-Azevedo, B., Jamerson, M., Cabral, G.A., Silva-Filho, F.C., Marciano-Cabral, F., 2009.
545 *Acanthamoeba* interaction with extracellular matrix glycoproteins: Biological and biochemical
546 characterization and role in cytotoxicity and invasiveness. J. Eukaryot. Microbiol. 56, 270–278.
547 Day, C.J., Tiralongo, J., Hartnell, R.D., Logue, C.A., Wilson, J.C., von Itzstein, M., Korolik, V., 2009.
548 Differential carbohydrate recognition by *Campylobacter jejuni* strain 11168: Influences of
549 temperature and growth conditions. PLoS One. 4, e4927.
550 de Koning, H.P., 2017. Drug resistance in protozoan parasites. Emerg. Top. Life Sci. 1, 627–632.
551 English, Chloe J., Tyml, T., Botwright, N.A., Barnes, A.C., Wynne, J.W., Lima, P.C., Cook, M.T., 2019. A
552 diversity of amoebae colonise the gills of farmed Atlantic salmon (*Salmo salar*) with amoebic gill
553 disease (AGD). Eur. J. Protistol. 67, 27–45.
554 English, C.J., Botwright, N.A., Adams, M.B., Barnes, A.C., Wynne, J.W., Lima, P.C., Cook, M.T., 2021.
555 Immersion challenge of naïve Atlantic salmon with cultured *Nolandella* sp. and *Pseudoparamoeba* sp.
556 did not increase the severity of *Neoparamoeba perurans* -induced amoebic gill disease (AGD). J. Fish
557 Dis. 44, 149–160.
558
559 Frederick, J.R., Petri, W.A., 2005. Roles for the galactose-/N-acetylgalactosamine-binding lectin of
560 Entamoeba in parasite virulence and differentiation. Glycobiology 15, 53-59.
561 Gandhi, N.S., Mancera, R.L., 2008. The structure of glycosaminoglycans and their interactions with proteins.
562 Chem. Biol. Drug Des. 72, 455–482.

563 Garate, M., Marchant, J., Cubillos, I., Cao, Z., Khan, N.A., Panjwani, N., 2006. In vitro pathogenicity of
564 Acanthamoeba is associated with the expression of the mannose-binding protein. Investig.
565 Ophthalmol. Vis. Sci. 47, 1056–1062.
566 Gilchrist, C.A., Petri, W.A.J., 1999. Virulence factors of Entamoeba. Curr. Opin. Microbiol. 2, 433–437.
567 Hu, S., Wong, D.T., 2009. Lectin microarray. Proteomics Clin. Appl. 3, 148–154.
568 Huang, M.L., Cohen, M., Fisher, C.J., Schooley, R.T., Gagneux, P., Godula, K., 2015. Determination of
569 receptor specificities for whole influenza viruses using multivalent glycan arrays. Chem. Commun.
570 51, 5326–5329.
571 Huth, S., Reverey, J.F., Leippe, M., Selhuber-Unkel, C., 2017. Adhesion forces and mechanics in mannose-
572 mediated acanthamoeba interactions. PLoS One 12, 1–14.
573 Imbert-Bouyer, S., Merlaud, A., Imbert, C., Daniault, G., Rodier, M.H., 2004. A mannose binding protein is
574 involved in the adherence of *Acanthamoeba* species to inert surfaces. FEMS Microbiol. Lett. 238,
575 207–211.
576 Jamerson, M., da Rocha-Azevedo, B., Cabral, G.A., Marciano-Cabral, F., 2012. Pathogenic *Naegleria*
577 *fowleri* and non-pathogenic *Naegleria lovaniensis* exhibit differential adhesion to, and invasion of,
578 extracellular matrix proteins. Microbiology 158, 791–803.
579 Kim, H.S., Hyun, J.Y., Park, S.H., Shin, I., 2018. Analysis of binding properties of pathogens and toxins
580 using multivalent glycan microarrays. RSC Adv. 8, 14898–14905.
581 Kollmann, D., Nagl, B., Ebner, C., Emminger, W., Wöhrl, S., Kitzmüller, C., Vrtala, S., Mangold, A.,
582 Ankersmit, H.J., Bohle, B., 2017. The quantity and quality of α-gal-specific antibodies differ in
583 individuals with and without delayed red meat allergy. Allergy Eur. J. Allergy Clin. Immunol. 72,
584 266–273.
585 Lamotte, S., Späth, G.F., Rachidi, N., Prina, E., 2017. The enemy within: Targeting host–parasite interaction
586 for antileishmanial drug discovery. PLoS Negl. Trop. Dis. 11, 1–14.
587 Leher, H., Silvany, R., Alizadeh, H., Huang, J., Niederkorn, J.Y., 1998. Mannose induces the release of
588 cytopathic factors from *Acanthamoeba castellanii*. Infect. Immun. 66, 5–10.
589 Lima, P.C., Taylor, R.S., Cook, M., 2017. Pseudocyst formation in the marine parasitic amoeba
590 *Neoparamoeba perurans*: a short-term survival strategy to abrupt salinity variation. J. Fish Dis. 40,
591 1109–1113.

592 Liu, Y., McBride, R., Stoll, M., Palma, A.S., Silva, L., Agravat, S., Aoki-Kinoshita, K.F., Campbell, M.P.,
593 Costello, C.E., Dell, A., Haslam, S.M., Karlsson, N.G., Khoo, K.-H., Kolarich, D., Novotny, M. V,
594 Packer, N.H., Ranzinger, R., Rapp, E., Rudd, P.M., Struwe, W.B., Tiemeyer, M., Wells, L., York,
595 W.S., Zaia, J., Kettner, C., Paulson, J.C., Feizi, T., Smith, D.F., 2016. The minimum information
596 required for a glycomics experiment (MIRAGE) project: improving the standards for reporting
597 glycan microarray-based data. Glycobiology. 27, 280-284.
598 Loomis, W.F., Fuller, D., Gutierrez, E., Groisman, A., Rappel, W.J., 2012. Innate non-specific cell
599 substratum adhesion. PLoS One. 7, e42033.
600 Macher, B.A., Galili, U., 2008. The Galα1,3Galβ1,4GlcNAc-R (α-Gal) epitope: A carbohydrate of unique
601 evolution and clinical relevance. Biochim. Biophys. Acta - Gen. Subj. 1780, 75–88.
602 Marcos-López, M., Espinosa Ruiz, C., Rodger, H.D., O'Connor, I., MacCarthy, E., Esteban, M.Á., 2017.
603 Local and systemic humoral immune response in farmed Atlantic salmon (*Salmo salar* L.) under a
604 natural amoebic gill disease outbreak. Fish Shellfish Immunol. 66, 207–216.
605 Martin, R.E., 1987. Adhesion, morphology, and locomotion of *Paramoeba pemaquidensis* Page (Amoebida,
606 Paramoebidae): Effects of substrate charge density and external cations1. J. Protozool. 34, 345–349.
607 Mitchell, S.O., Rodger, H.D., 2011. A review of infectious gill disease in marine salmonid fish. J. Fish Dis.
608 34, 411–432.
609 Morrison, R.N., Cooper, G.A., Koop, B.F., Rise, M.L., Bridle, A.R., Adams, M.B., Nowak, B.F., 2006.
610 Transcriptome profiling the gills of amoebic gill disease (AGD)-affected Atlantic salmon (*Salmo*
611 *salar* L.): A role for tumor suppressor p53 in AGD pathogenesis? Physiol. Genomics 26, 15–34.
612 Niimura, Y., 2006. Isolation and characterization of acidic glycosphingolipids from the gill of the Pacific
613 Salmon (*Oncorhynchus keta*): A novel hybrid-type ganglioside with isoglobo- and neolacto-Series.
614 Glycoconj. J. 23, 651–661.
615 Nowak, B., Valdenegro-Vega, V., Crosbie, P., Bridle, A., 2014. Immunity to amoeba. Dev. Comp. Immunol.
616 43, 257–267.
617 Oldham, T., Rodger, H., Nowak, B.F., 2016. Incidence and distribution of amoebic gill disease (AGD) - An
618 epidemiological review. Aquaculture 457, 35–42.
619 Panjwani, N., 2010. Pathogenesis of *Acanthamoeba keratitis*. Ocul. Surf. 8, 70–79.

Parsons, H., Nowak, B., Fisk, D., Powell, M., 2001. Effectiveness of commercial freshwater bathing as a treatment against amoebic gill disease in Atlantic salmon. Aquaculture 195, 205–210.

Pendrill, R., Mutter, S.T., Mensch, C., Barron, L.D., Blanch, E.W., Popelier, P.L.A., Widmalm, G., Johannessen, C., 2019. Solution structure of mannobioses unravelled by means of raman optical activity. Chem. Phys. Chem. 20, 695–705.

Raval, Y.S., Stone, R., Fellows, B., Qi, B., Huang, G., Mefford, O.T., Tzeng, T.R.J., 2015. Synthesis and application of glycoconjugate-functionalized magnetic nanoparticles as potent anti-adhesion agents for reducing enterotoxigenic *Escherichia coli* infections. Nanoscale 7, 8326–8331.

Ravdin, J.I., Guerrant, R.L., 1981. Role of adherence in cytopathogenic mechanisms of *Entamoeba Histolytica*. J. Clin. Invest. 68, 1305–1313.

Ravdin, J.I., John, J.E., Johnston, L.I., Innes, D.J., Guerrant, R.L., 1985. Adherence of *Entamoeba histolytica* trophozoites to rat and human colonic mucosa. Infect. Immun. 48, 292–297.

Ravdin, J.I., Petri, W.A., Murphy, C.F., Smith, R.D., 1986. Production of mouse monoclonal antibodies which inhibit in vitro adherence of *Entamoeba histolytica* trophozoites. Infect. Immun. 53, 1–5.

Reverter, M., Tapissier-Bontemps, N., Lecchini, D., Banaigs, B., Sasal, P., 2018. Biological and ecological roles of external fish mucus: A review. Fishes 3, 1–19.

Sarabia-Sainz, H.M., Armenta-Ruiz, C., Sarabia-Sainz, J.A.I., Guzmán-Partida, A.M., Ledesma-Osuna, A.I., Vázquez-Moreno, L., Montfort, G.R.C., 2013. Adhesion of enterotoxigenic *Escherichia coli* strains to neoglycans synthesised with prebiotic galactooligosaccharides. Food Chem. 141, 2727–2734.

Semchenko, E.A., Moutin, M., Korolik, V., Tiralongo, J., Day, C.J. 2012. Lectin array analysis of purified lipooligosaccharide: A method for the determination of molecular mimicry. J Glycomics Lipidomics 2, 1-5.

Singh, R.S., Walia, A.K., Kanwar, J.R., 2016a. Protozoa lectins and their role in host–pathogen interactions. Biotechnol. Adv. 34, 1018–1029.

Singh, R.S., Walia, A.K., Kanwar, J.R., Kennedy, J.F., 2016b. Amoebiasis vaccine development: A snapshot on *Entamoeba histolytica* with emphasis on perspectives of Gal/GalNAc lectin. Int. J. Biol. Macromol. 91, 258–268.

Smith, D.F., Cummings, R.D., 2014. Investigating virus-glycan interactions using glycan microarrays. Curr. Opin. Virol. 7, 79–87.

649 Valdenegro-Vega, V.A., Crosbie, P.B.B., Cook, M.T., Vincent, B.N., Nowak, B.F., 2014. Administration of
650 recombinant attachment protein (r22C03) of *Neoparamoeba perurans* induces humoral immune
651 response against the parasite in Atlantic salmon (*Salmo salar)*. Fish Shellfish Immunol. 38, 294–302.
652 Weli, S.C., Aamelfot, M., Dale, O.B., Koppang, E.O., Falk, K., 2013. Infectious salmon anaemia virus
653 infection of Atlantic salmon gill epithelial cells. Virol. J. 10, 5.
654 Wright, D.W., Nowak, B., Oppedal, F., Crosbie, P., Stien, L.H., Dempster, T., 2018. Repeated sublethal
655 freshwater exposures reduce the amoebic gill disease parasite, *Neoparamoeba perurans*, on Atlantic
656 salmon. J. Fish Dis. 41, 1403–1410.
657 Yamada, S., Sugahara, K., Özbek, S., 2011. Evolution of glycosaminoglycans: Comparative biochemical
658 study. Commun. Integr. Biol. 4, 150–158.
659 Yan, L., Xia, K., Yu, Y., Miliakos, A., Chaturvedi, S., Zhang, F., Chen, S., Chaturvedi, V., Linhardt, R.J.,
660 2020. Unique cell surface mannan of yeast pathogen *Candida auris* with selective binding to IgG.
661 ACS Infect. Dis. 6, 1018–1031.
662 Yang, Z., Cao, Z., Panjwani, N., 1997. Pathogenesis of *Acanthamoeba keratitis*: Carbohydrate-mediated
663 host- parasite interactions. Infect. Immun. 65, 439–445.
664 Yu, R.K., Tsai, Y.-T., Ariga, T., Yanagisawa, M., 2011. Structures, biosynthesis, and functions of
665 gangliosides - an overview. J. Oleo Sci. 60, 537–544.

Legend to Figures

Fig. 1. Labelling confirmation of parasitic amoeba *Neoparamoeba perurans* and Atlantic salmon (*Salmo salar*) gill cells for glycan and lectin microarrays. Flow cytometric histograms of labelled (left peak) and unlabelled (right peak) cells of (A) amoeba, (B) pseudocysts, and (C) gill epithelia. All three cells were successfully labelled using Bodipy595-ME dye.

Fig. 2. In vitro solid-phase adherence and competitive assays. (A) The abundance of metabolically available *Neoparamoeba perurans* trophozoites attached to mannobiose-BSA, *N*-acetylgalactosamine-BSA (GalNAc-BSA) and BSA-only-coated wells, following 2 h incubation. The assay was repeated in the presence of free mannose or GalNAc to assess the ability of these glycans to binding to the amoeba surface and, therefore, block the observed glycan-mediated binding. A free sucrose treatment was included as a control. RLU, relative light unit. (B) Phase-contract images illustrating the remaining attached trophozoites at the end of the 2 h incubation period (x10 objective, scale bar 50 μm).

Highlights

- Glycan-lectin interactions between *Neoparamoeba perurans* and the host were explored
- Glycan and lectin arrays were employed in amoeba and gill cells, respectively
- A series of glycans bound by the amoeba were also detected on gill epithelial cells
- Mannobiose and *N*-acetylgalactosamine showed the strongest binding affinity
- Increased binding was seen on mannobiose and *N*-acetylgalactosamine-coated surfaces

Table 1. Heat map indicating the commercial lectins immobilised on the lectin microarray and their respective binding specificity. Highlighted in grey are the lectins successfully bound by labelled gill cells of Atlantic salmon (*Salmo salar*).

Glycan	Array	Abbreviation	Binding specificity
Fucose		AAA	Fucα1-2
		LAL	Fuc?
		Lotus	Fucα1-2, Galβ1-4(Fucα1-3)GlcNAc
		RSL	Fucα1-2Gal
		UEA-I	Fucα

	PA-IIL	Fuc
Beta galactose	ABA	Galβ1-3GalNAc
	ACA	Galβ1-3GalNAc
	AMA	Galβ1-4GlcNAc
	CA	Galβ1-4GlcNAc, GalNAcβ1-4GlcNAc
	ECA	Galβ1-4GlcNAc (Terminal)
	PHA-E	Galβ1-4GlcNAcβ1-2(Galβ1-4GlcNAcβ1-6)Man
	PHA-L	Galβ1-4GlcNAcβ1-2Man
	PNA	Galβ1-4Glc, Gal (Terminal)
	SNA-II	Galβ (Terminal), GalNAcβ (Terminal)
	TKA	Galβ, Galβ1-4Glc (Lactose)
	VAA	Galβ
	VGA	Galβ1-3GalNAc
Mannose	ASA	Manα1-3
	Calsepa	Man, Glc, Glcα1-4Glc
	ConA	Man (Terminal, Branched), GlcNAc (Terminal)
	CPA	Manα? Man?
	GNA	Manα1-3Man (Terminal)
	HHA	Manα1-3/6 (Terminal)
	LcH	complex (Man/GlcNAc core with Fuca1-6)
	LcH B	α-Man> a-Glc, GlcNAc
	MNA-M	Manα
	NPA	Manα? Manβ?
	PEA, PSA	Manα, Glcα, GlcNAcα
	PMA	Manα1-3
	Succinyl Con A	Manα, Glcα
	VFA	Manα, Glc, GlcNAc
	VVA Man	Man
	BC2LA	Man
N`acetylgalactosamine	BDA	GalNAcα, GalNAcβ
	BPA	GalNAc
	CSA	GalNAcα (Terminal)
	DBA	GalNAcα1-3GalNAc, GalNAcα1-3Gal
	GS-1-A4	GalNAcα
	HMA	GalNAcα, Fucα, Neu5Ac
	HPA	GalNAcα (Terminal)
	IAA	GalNAc
	IRA	GalNAcα1-3Galβ
	LBA	GalNAcα, GalNAcα1-3(Fucα1-2)Gal
	PTA GalNAc	GalNAc
	RPA	GalNAc
	SBA	GalNAcα (Terminal), Neu5Acα2-6GalNAc (Tn antigen)
	SHA	GalNAc
	SJL	GalNAc > Gal
	SSA	GalNAc, Terminal, O-link
	TL	α-GalNAc,β-GalNAc, GalNAc, Gal, Fucose

		VVA	GalNAcα, GalNAcα1-3Gal
		WFA	GalNAcα, GalNAcβ
		CDA	GalNAcα
		EEA	GalNAcβ
Alpha galactose		BS-1	Galα
		GHA	Galα, GalNAcα
		GS-1-B4	Galα (Terminal)
		JACLIN	Galα, Galβ, GalNAcα (O-linkage)
		MNA-G	Galα, Galβ
		MOA	Galα1-3
		MPA	Galα, Galα1-6Glc, Galβ1-6GalNAcα
		PTA Galactose	Gal
		VRA	Galα,
		PA-IL	Gal
N`Acetylglucosamine		CAA	GlcNAcβ1-2Manα1-3(GlcNAcβ1-2Manα1-6)Manβ1-4GlcNAcβ1-4GlcNAcβ
		GS-11	GlcNAcα, GlcNAcβ
		HAA	GlcNAcα, GalNAcα
		LAA	GlcNAcβ, GlcNAcβ1-4GlcNAc
		LEA	GlcNAc-β1,4GlcNAc
		PWM, PWA	GlcNAcβ1-4GlcNAc
		STA	[GlcNAcβ1-4]3 GlcNAc > [GlcNAcβ1-4]2 GlcNAc > GlcNAcβ1-4 GlcNAc
		Succinyl WGA	[GlcNAcβ1-4]2
		UDA	GlcNAcβ
		UEA-II	GlcNAcβ1-4GlcNAc
		WGA	GlcNAcβ
Sialic acid		CCA	Neu5Ac
		LFA	Neu5Ac, Neu5Gc
		LPA	Neu5Ac, Neu5Gc
		MAA	Neu5Acα2-3Gal
		PSL	Neu5Acα2-6Galβ1-4GlcNAc, Neu5Acα2-6Galβ1-4Glc
		SNA-I	Neu5Acα2-6Gal, Neu5Acα2-6GalNAc
Glucose		RTA	Glc?
Complex		PHA-M	complex
		PHA-P	complex
Unknown		PAA	unknown
		MIA	unknown

Table 2. Glycans selected to assess binding interactions with the surface of *Neoparamoeba perurans* by surface plasmon resonance (SPR), and their respective structure, dissociation equilibrium constant (K_D), predicted maximum binding response (R_{max}) and chi^2 values.

696

ID	Structure	K_D (M)	R_{max} (RU)	chi^2
1A	Galβ1-3GlcNAc	3.04E-07 ± 3.50E-07	1.8 ± 0.4	0.134
1E	Galβ1-3GalNAc	5.97E-08 ± 5.20E-08	5.2 ± 1.0	0.722
7I	Galβ1-4(Fucα1-3)GlcNAc	1.06E-07 ± 7.60E-08	6.0 ± 1.0	0.735
19J	Galβ1-4(Fucα1-3)GlcNAcβ1-3Gal	2.16E-08 ± 1.60E-08	4.5 ± 0.7	0.266
10B	Neu5Acα2-3Galβ1-4(Fucα1-3)GlcNAc	3.23E-08 ± 2.20E-08	5.1 ± 0.7	0.342
17G	Neu5Acα2-3Galβ1-3GalNAcβ1-4Galβ1-4Glc	6.56E-08 ± 6.90E-08	4.8 ± 1.1	0.934
17N	Neu5Acα2-8Neu5Acα2-3Galβ1-4Glc	6.91E-08 ± 7.70E-08	5.7 ± 1.4	1.49
5D	Manα1-3Man	1.24E-08 ± 3.00E-09	1.4 ± 0.1	0.0302
5E	Manα1-4Man	1.22E-07 ± 5.70E-08	5.4 ± 0.6	0.246
5F	Manα1-6Man	1.14E-07 ± 1.60E-07	2.1 ± 0.6	0.309
2C	GalNAcβ1-3Gal	8.97E-09 ± 3.60E-09	4.7 ± 0.5	0.0935
7F	Fucα1-2Gal	1.13E-07 ± 5.80E-08	2.1 ± 0.2	0.0423
7K	GalNAcα1-3(Fucα1-2)Gal	1.21E-07 ± 1.00E-07	3.1 ± 0.6	0.277
8P	GalNAcα1-3(Fucα1-2)Galβ1-4GalNAc	NB	NB	NB
20B	GalNAcα1-3(Fucα1-2)Galβ1-3GalNAcβ1-3Gal	1.25E-07 ± 1.00E-07	3.9 ± 0.8	0.471
18E	GalNAcα1-3(Fucα1-2)Galβ1-4(Fucα1-3)Glc	1.26E-07 ± 1.20E-07	4.0 ± 0.8	0.517
7O	Fucα1-2Galβ1-3GlcNAc	1.74E-08 ± 1.10E-08	4.3 ± 0.6	0.189

697 ID, identity; related names are found in Supplementary Table S1.
698 RU, response unit.
699 NB, no binding.
700

701 Table 3. Heat map indicating the identity (ID) of glycans immobilised on the glycan microarray. Highlighted
702 in grey are those successfully bound by labelled *Neoparamoeba perurans* amoebae (A) and pseudocysts (P).
703 Glycans are grouped according to their main classes and their common names and structures can be found in
704 Supplementary Table S1.

Glycan	ID	A	P	Glycan	ID	A	P	Glycan	ID	A	P	Glycan
Monosaccharides	1			**Terminal Galactose**	75			**Fucosylated**	71			**Sialylated**
	2				76				72			
	3				77				73		■	
	4				78	■			215			
	5				80				216			
	6				81				217			
	7				83	■			219			
	9				84				226		■	
	10				85				233			
	14				87	■			234			
	15				88				235		■	
	16				89				287		■	
	18	■			93				288		■	
	19				94				359			
	20				97	■			360			
	22				100	■			362		■	
	37				145	■			363			
	38				146				364			

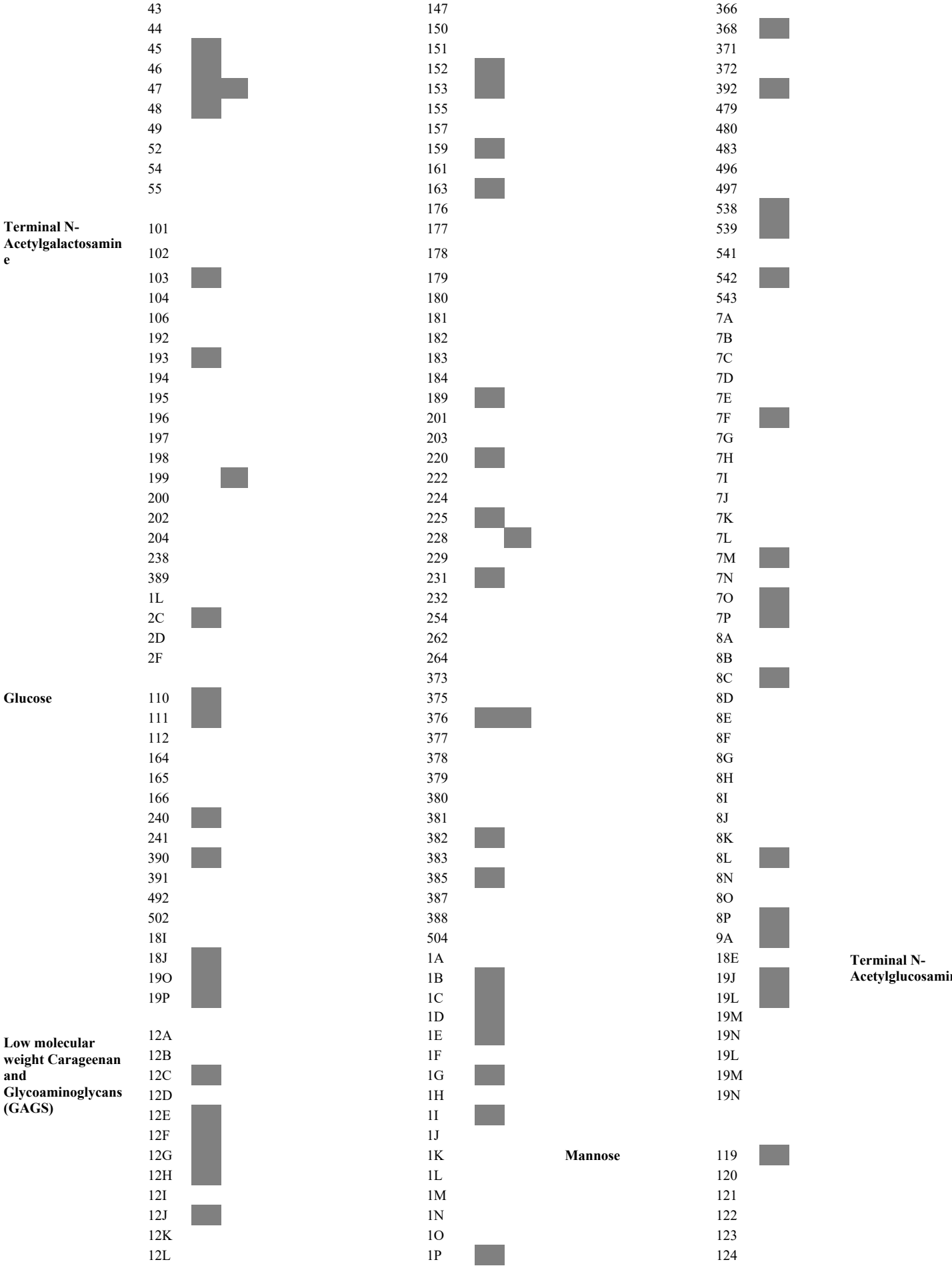
43
44
45
46
47
48
49
52
54
55
Terminal N-Acetylgalactosamine
101
102
103
104
106
192
193
194
195
196
197
198
199
200
202
204
238
389
1L
2C
2D
2F
Glucose
110
111
112
164
165
166
240
241
390
391
492
502
18I
18J
19O
19P
Low molecular weight Carageenan and Glycoaminoglycans (GAGS)
12A
12B
12C
12D
12E
12F
12G
12H
12I
12J
12K
12L
147
150
151
152
153
155
157
159
161
163
176
177
178
179
180
181
182
183
184
189
201
203
220
222
224
225
228
229
231
232
254
262
264
373
375
376
377
378
379
380
381
382
383
385
387
388
504
1A
1B
1C
1D
1E
1F
1G
1H
1I
1J
1K
1L
1M
1N
1O
1P
366
368
371
372
392
479
480
483
496
497
538
539
541
542
543
7A
7B
7C
7D
7E
7F
7G
7H
7I
7J
7K
7L
7M
7N
7O
7P
8A
8B
8C
8D
8E
8F
8G
8H
8I
8J
8K
8L
8N
8O
8P
9A
18E
19J
19L
19M
19N
19L
19M
19N
Mannose
119
120
121
122
123
124
Terminal N-Acetylglucosamin

	12M			2A		258	
	12N			2B		495	
	12O			2F		5A	
	12P			2G		5B	
	13A			18B		5C	
	13B			18C		5D	
	13C			18L		5E	
	13D			18M		5F	
	13E			18N		5G	
						5H	
High molecular weight Carageenan and Glycoaminoglycans (GAGS)	625		**Gangliosides**	17A			
	13F			17B		**Complex N-glycans**	627
	13G			17C			19A
	13H			17D			19B
	13I			17E			19C
	13J			17F			19D
	13K			17G			19E
	13L			17H			
	13M			17I			
	13N			17J			
	130			17K			
	13P			17L			
	14B			17M			
	14C			17N			
	14D			17O			
	14E			17P			
	14F						
	14G						
	14H						
	14I						
	14J						
	14K						

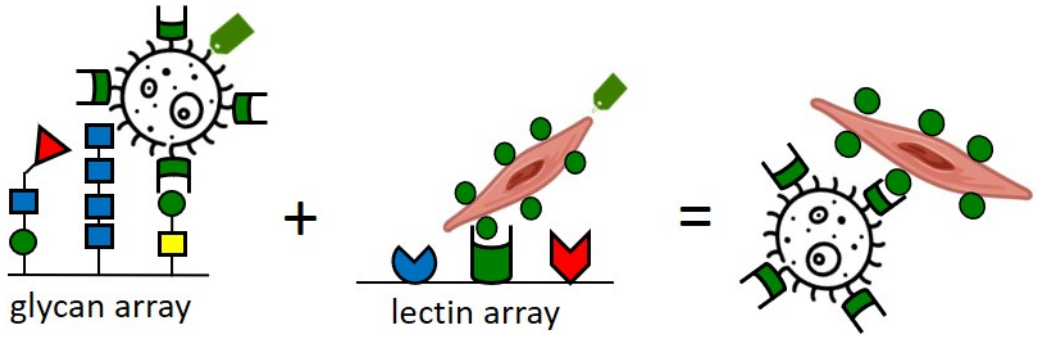

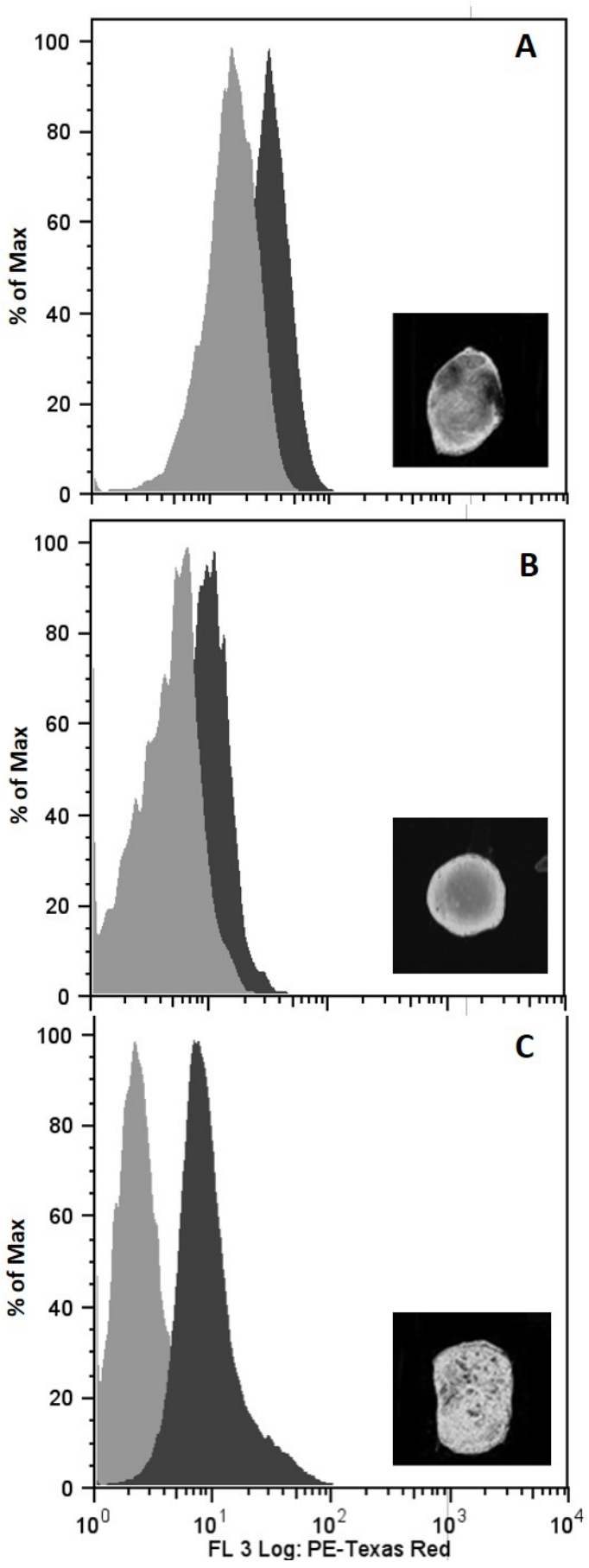
A
B
C
% of Max
100
80
60
40
20
0
10^0
10^1
10^2
10^3
10^4
FL 3 Log: PE-Texas Red

708

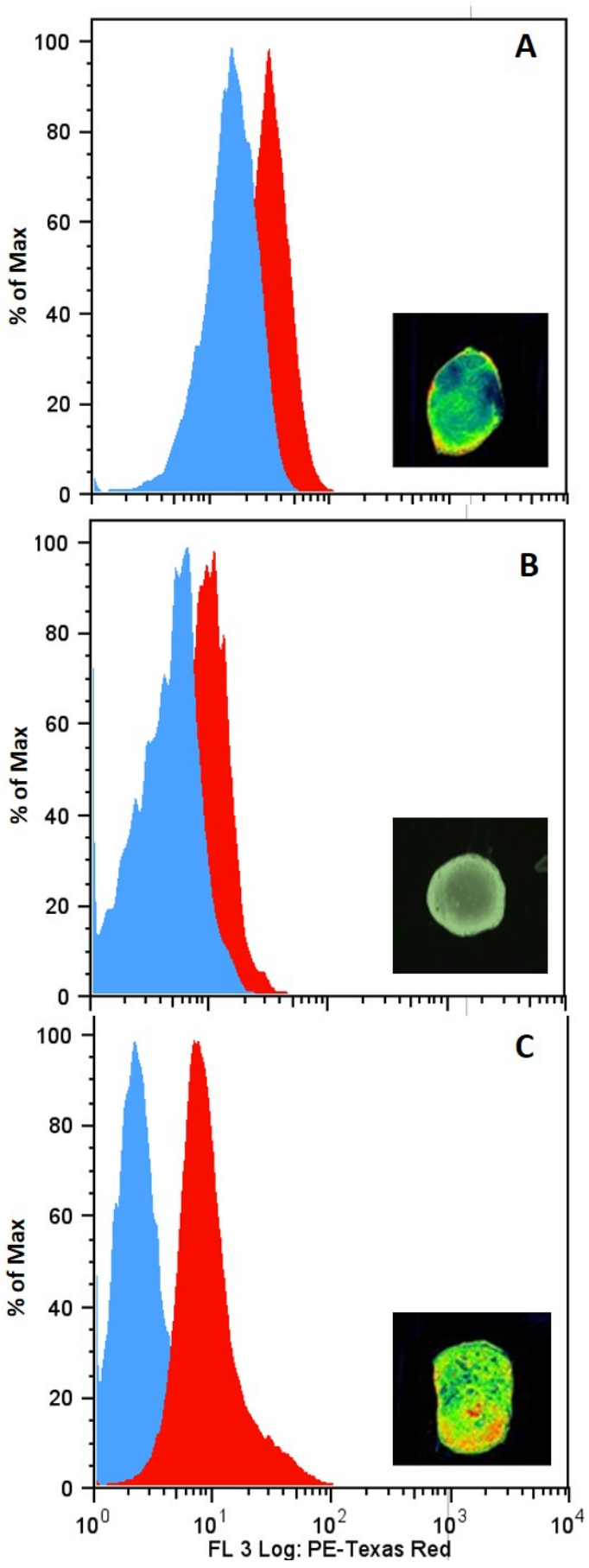
A
B
C
% of Max
100
80
60
40
20
0
10^0
10^1
10^2
10^3
10^4
FL 3 Log: PE-Texas Red

709

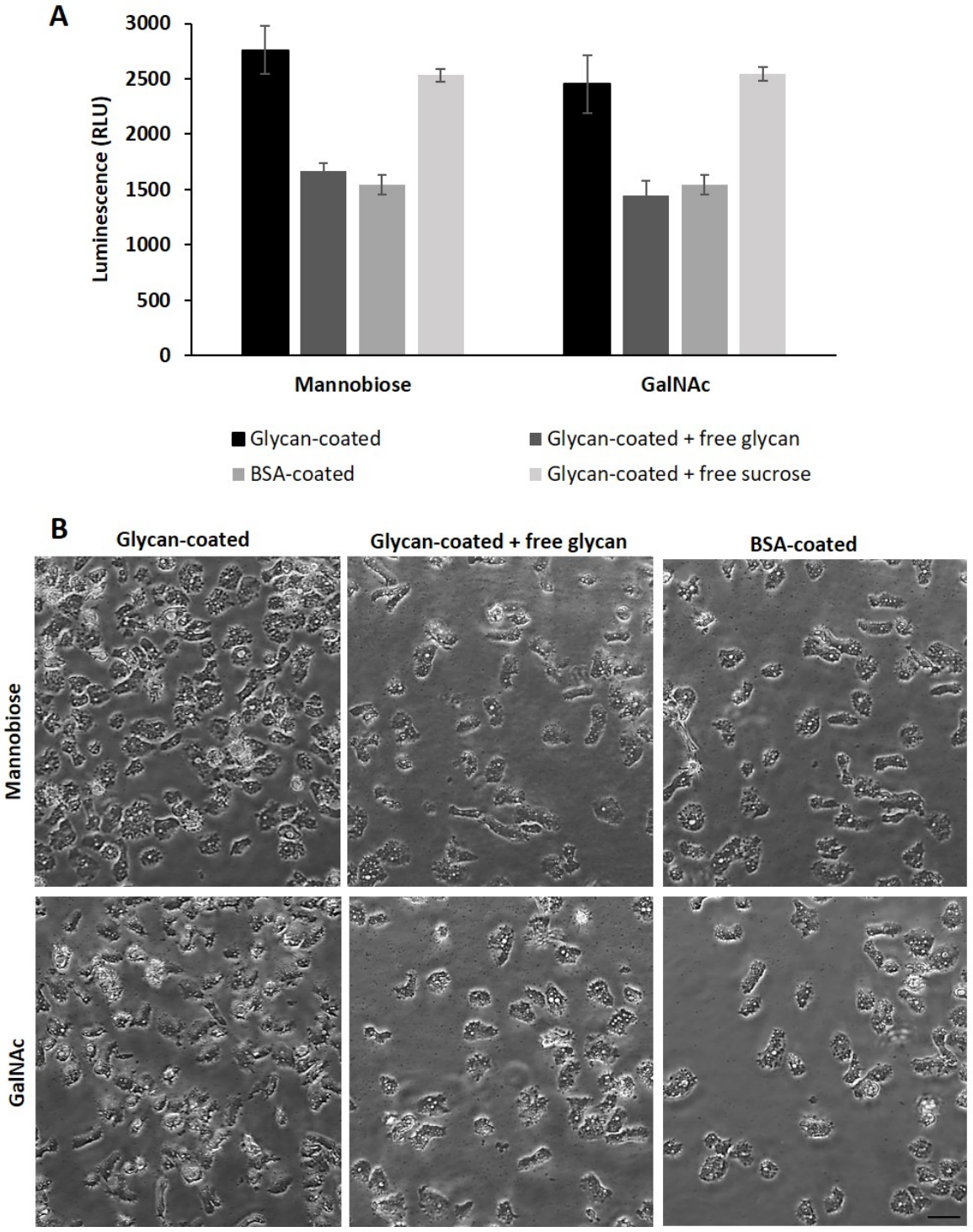
A
3000
2500
2000
1500
1000
500
0
Luminescence (RLU)
Mannobiose
GalNAc
Glycan-coated
Glycan-coated + free glycan
BSA-coated
Glycan-coated + free sucrose
B
Glycan-coated
Glycan-coated + free glycan
BSA-coated
Mannobiose
GalNAc

710